

## **Corrosion Resistance of Stainless Steels Exposed to Aggressive Environments with Particles and Water**

H. Tsaprailis, W. Kovacs III, J. Tuggle & L. F. Garfias-Mesias\*  
DNV/CC Technologies, Inc.

Corrosion and Materials Technology Laboratory  
5777 Frantz Road, Dublin, OH 43017-1386 USA  
Tel: +1 (614) 761-1214

\*E-mail: [Luis.Garfias@DNV.com](mailto:Luis.Garfias@DNV.com)

### **ABSTRACT**

The present work describes the corrosion studies (using electrochemical techniques) of coated and uncoated steels exposed to corrosive mixtures (including 6% ferric Chloride, alcohols, particles and water). Open Circuit Potential (OCP), Cyclic Potentiodynamic Polarization (CPP) and a modified version of the Zero Resistance Amperometry (ZRA) testing methodology were proposed to compare the corrosion resistance of several steel exposed to these environments.

The modified version of the ZRA is not only measured accurately (within 1°C) the Critical Pitting Temperature (CPT) on the different alloys studied (metallic bars exposed to 6% Ferric Chloride), but also allowed to perform the testing in a very short time. This technique is a promising way to characterize and rank different materials subjected to the same environmental conditions.

The CPP tests in 316 SS showed that the addition of the sand decreased the Pitting Potential in 316 Stainless Steels by about 130 mV<sub>SCE</sub>. However, in the 25-Cr DSS the only effect observed was an increase in the passive current (no pitting was observed at this temperature). The abrasion testing of different coated steels in 3.5% NaCl with and without additions of sand particles at very high speed (rotation experiment) was used to characterize the coating performance in these environments. As expected, the carbon steels presented very high currents (thousands of microAmps) once the coating was compromised (after the rotation started). Similarly, the Stainless Steels (SS) type 303 and 316 showed high currents (hundreds of microAmps) once the coating was compromised (after the rotation started). When the same coating (Epoxy A) is applied to 304 SS sample, exposed to a mixture of 90% Mono-Ethylene Glycol and 10% deionized water (DI H<sub>2</sub>O) (without rotation) and increased the temperature, the coating breaks down at higher temperatures (increase in the current and drop in the potential measured). Ongoing work is aiming at understanding what is the critical temperature and rotational speed for these types of coatings.

### **INTRODUCTION**

Recently, due to the increasingly high demand for oil, drilling in deeper and harsher environments had opened a window of opportunities to existing engineering materials exposed to more aggressive environments. New methodologies are being developed to assess the risk for failure of coated carbon steels, coated and uncoated arsenic stainless steels (SS) and uncoated highly alloyed steels. The main objective is to predict the performance of these materials in very harsh applications. A thorough understanding of the corrosion properties of these materials exposed to these complex fluids (mixtures of fluids that include corrosive agents and particulates) is desirable to facilitate safety, long service life and design of equipment.

Copyright

©NACE International. All rights reserved. Paper Number 09277 reproduced with permission from CORROSION 2009 Annual Conference and Exhibition, Atlanta.

Inexpensive carbon steels and austenitic stainless steels (type 304 and 316) are the typical choice for most industries to produce components for downhole applications. However, in harsher conditions, Duplex Stainless Steels (DSS) as well as highly alloyed steels (including Ni alloys) are typically used to guarantee longer service life. However, any materials containing Ni is currently in high demand and therefore every attempt is made to limit the amount of Ni in any material that needs it for harsh environment.

In the present work, the development of two novel methodologies to assess the pitting corrosion and wear resistance of steels exposed to aggressive environments are described.

### **Critical Pitting Temperature Determination**

The first method involves the determination of the Critical Pitting Temperature (or CPT)<sup>1</sup>. The CPT is defined briefly in the next few sentences. Below the CPT no stable pitting corrosion should occur (in a similar environment). Near the CPT, metastable pits may develop but would repassivate<sup>2</sup>. Once the CPT is reached, metastable pits will develop into stable pits<sup>3</sup>.

Traditionally, the CPT determination is made by using the ASTM G48 method<sup>1</sup>. This method consists of exposing several samples for over 72 hours to a solution containing 6% ferric chloride at a given temperature followed by weight measurements. If no significant amount of weight is lost, then a new set of samples is exposed at 5°C higher than in the previous test. This is repeated several times until a significant change in the weight of the coupons is found. This method is fairly accurate, but tedious and time consuming.

A second type of CPT determination was suggested by Salinas-Bravo and Newman<sup>4</sup>. In their pioneer work, Salinas-Bravo and Newman suggested that by coupling two similar samples from the same material, through a zero resistance ammeter (ZRA), the current flowing between the two samples will increase 'abruptly' when pitting starts (while the solution is being heated above the CPT). Salinas-Bravo and Newman used this methodology to determine the CPT of two duplex stainless steels at different compositions. However, Salinas-Bravo and Newman used fast heating rates, which could lead to higher CPT values.

A third type of CPT determination is found in the ASTM G150 test method<sup>5</sup>. This method suggests the use of a conventional three-cell electrode to determine the CPT. Additionally, it requires that the sample (working electrode) needs to be polarized to 700 mV<sub>SCE</sub>.

In the present work, a modified version of the test methodology suggested by Salinas-Bravo and Newman<sup>4</sup> are proposed. The main improvements to their work can yield a more accurate CPT and at the same time, facilitate the experimental design avoiding crevices in the samples studied.

### **Rotational Abrasion Testing and Corrosion Monitoring**

The effect of flow on the corrosion resistance of steel coated under harsh mixtures (that contains a mixture of liquids and particulates) was also studied. The main objective of this testing methodology consists on mimicking the flow conditions of high speed downhole rotating components. Additionally, wear and coating disbonding resulting from the impact of the particles on the surface of the samples can be monitored (in real time). This approach has some similarities to the conventional rotating cylinder and rotating cage approaches<sup>6</sup> (where the rotating cylinders can

reach speeds of up to 4,000 rpm), which has been used to determine the synergism between wear and corrosion<sup>7</sup>.

The present work shows the first attempt to use a motor that rotates a cylinder which can reach very high surface velocities (from ~12,000 rpm to ~22,000 rpm) with simultaneous monitoring of the current and potential in the cell. This configuration allows monitoring (electrochemically) the coating failure while the samples are exposed to a mixture of liquids and particulates. The first part of the experimental section will include results on conventional steels, coated with two types of proprietary epoxies immersed in a mixture of 3.5% NaCl and sand while the samples are stagnant (not rotated), rotated at the minimum and maximum speeds (~12,000 and ~22,000 rpm).

## EXPERIMENTAL

### Materials

Table 1 shows the composition of the alloys used in the present work to determine the CPT. The samples were supplied in a form of a bar approximately 10 mm in diameter. The outer part of the bar was removed after annealing by machining to produce samples in the form of rods 8.5 mm in diameter. The end face of each rod (the surface to be tested) was carefully machined to give a smooth finish and further wet ground to 4000 mesh finish then degreased in acetone, followed by a rinsing in isopropyl alcohol and drying with pure nitrogen. The chemical compositions of the different phases were detected by using a Cameca SEMPROBE at a current of 10  $\mu$ A at 20 KeV. Analysis was made at intervals of 2  $\mu$ m.

Table 2 shows the steels used in the present work for rotation studies. All the steels were supplied in a form of a bar 0.5 inches in diameter and 12 inches in length. The bars were degreased in acetone, followed by a rinsing in isopropyl alcohol and drying with pure nitrogen. Following the cleaning procedure, the bars were coated with epoxy A and B (see table 2). The approximate thickness of the coating was about 50 micrometers.

### Critical Pitting Temperature Determination

Critical Pitting Temperature (CPT) test was done using a method similar to the Zero Resistance Amperometry (ZRA) test suggested by Salinas-Bravo and Newman (reference 4). In this test, two similar stainless steel samples were connected through a sensitive picoammeter (Keithley 485). The potential of the couple was recorded against either a Standard Calomel Electrode (SCE) or an Ag/AgCl Reference Electrode. The test solution was 250 ml of 10% FeCl<sub>3</sub> prepared according to the ASTM G48 method in a glass cell. To avoid crevices, the cell was arranged to allow only the end face of both specimens touched and wetted by the liquid surface creating a meniscus (see Figure 1). This defined the area under test (no attack has ever been found on the sides of the bar), avoiding any crevices. A potential output from the picoammeter was used to record the current. The potential, current and temperature measured were all logged simultaneously on a PC by using a data bucket (Fluke Hydra 2635A). The criterion used to determine the CPT of the samples was the temperature at which the current increased steadily and at the same time the potential dropped to more negative values.

### Cyclic Potentiodynamic Polarization (CPP)

Potentiodynamic sweeps at room temperature (24°C) in a 3.5 % NaCl solution were carried out at a rate of 1 mVs<sup>-1</sup>. The tests were carried out in a glass three-electrode cell. In all experiments, the

rod under test was supported in a holder on the lid of the cell such that the end face just touched the surface of the test solution as described above. The counter electrode was a platinum wire, the reference electrode a saturated calomel electrode (SCE) at the same solution temperature; all potentials are given against the SCE. The potential at which the current density exceeded  $20 \mu\text{Acm}^{-2}$  was defined as the pitting potential,  $E_p$ .

### **Rotational Abrasion Testing and Corrosion Monitoring**

Rotational abrasion testing and corrosion monitoring was conducted on epoxy-coated carbon steels, Cr-coated carbon steels, 303 SS, and 316L SS rods in a media composed of 3.5 % NaCl and fine particulate sand (4:1 volume ratio). The samples were mounted within an "in-house" manufactured rotational drive shaft that was able to rotate the rods at 12,100 rpm and 22,100 rpm. The potential of the sample was monitored between the sample rod and a saturated calomel electrode (SCE), while the current was collected between the rod and a graphite counter electrode using a picoammeter (Keithley 485). The potential, current and temperature measured were all logged simultaneously on a PC by using a data bucket (Fluke Hydra 2635A).

### **Critical Temperature in MEG and water**

Experiments were also conducted on 304L SS samples in 90% MEG in 10% H<sub>2</sub>O (representative of MEG under down-hole operational conditions) to accelerate the degradation of the protective epoxy coatings and expose the underlying substrate (i.e., 304L SS). In short, the potential between the epoxy-coated 304L SS sample and a pseudo-reference electrode (AgCl wire) was monitored using a picoammeter (Keithley 485). Concurrently, the current between the two epoxy-coated 304L SS samples (with similar exposed areas) were recorded using a data bucket (Fluke Hydra 2635A), while the temperature of the MEG solution was increased from 22.5 °C to 93.5 °C at a rate of 0.5 °C/min using a water bath (NesLab RTE17). It should be stressed that the samples were not rotated in this part of the work.

## **RESULTS AND DISCUSSIONS**

### **Critical Pitting Temperature Determination**

Figure 2 shows the potential against the SCE and the galvanic current between the two electrodes (25 Cr DSS, UNS S32550) as a function of the temperature. The temperature was constantly raised at a heating rate of  $0.5^\circ\text{Cmin}^{-1}$ . The reason for choosing this heating rate will be discussed in the section below. When the samples were first coupled at  $-25^\circ\text{C}$  the galvanic current observed was very low, less than 1 microAmp (and constant). Similarly, the potential measured between the galvanic couple and the SCE was constant, about  $-500 \text{ mV}$ . At about  $38^\circ\text{C}$  there was a fluctuation on the potential accompanied by small fluctuation on the current (believed to be a metastable event). As the temperature increased to  $\sim 45^\circ\text{C}$ , larger transients in both the current and the potential started to appear. At the CPT ( $62.3^\circ\text{C}$ ) the current rapidly increased with a simultaneous shift of the potential in the negative direction (at this point stable pitting started). This simultaneous drop of potential and an increase in couple current indicate the onset of pitting which is used to define the CPT.

Figure 3 shows the CPT measurements of exactly the same samples (25 Cr DSS, UNS S32550) used in Figure 2 but repeated at 5 different heating rates (0.05, 0.5, 0.68, 0.7 and  $0.9^\circ\text{Cmin}^{-1}$ ). The red dotted lines denote  $1^\circ\text{C}$  separation. It is clear from this figure that doing the experiment at slow rate (below  $0.7^\circ\text{C}$ ) will lead to essentially the same CPT (around  $62^\circ\text{C}$ )<sup>8</sup>. However, once the heating

rate is increased, there is sharp rise in the CPT measured. This is in complete agreement with the test methodology established in the ASTM G48 and ASTM G150 methodologies as well with the suggestions by Salinas-Bravo and Newman<sup>1,4,5</sup>. Further studies using a heating rate of  $0.5^{\circ}\text{Cmin}^{-1}$  by one of the authors has shown consistency between three different types of testing (the modified ZRA test and CPP in both 3.5% NaCl and with 3.5% NaCl plus 1 m HCl)<sup>9</sup>.

Figures 4, 5 & 6 show exactly the same type of experiment as shown in Figure 2 (described above) to determine the CPT of three different DSS alloys. Figure 4 shows the CPT of a 22 Cr DSS (UNS S32205), which yields approximately  $53^{\circ}\text{C}$ . Figure 5 shows the CPT of a 25Cr DSS (UNS 32750) yielding a value of  $71^{\circ}\text{C}$  and finally, figure 6 shows the CPT obtained for a 25 Cr DSS (UNS 32760). Table 3 shows the summary table for all 4 materials. Since we have established that the resolution for this technique is roughly  $1^{\circ}\text{C}$  (from Figure 3), all values indicated in table one have been rounded to the closest digit.

This novel method which produce relatively easy and fast CPT determinations have been extended to highly alloyed stainless steels, highly corrosion resistant metallic coatings and other type of materials. Furthermore, it has been also used to determine the Critical Crevice Temperature (CCT) in very high corrosion resistance materials<sup>10</sup>.

### **Cyclic Potentiodynamic Polarization (CPP)**

Prior to the “Rotational Abrasion Testing and Corrosion Monitoring” of some of the coated steels shown in Table 3, it was necessary to understand the role of the addition of sand to a solution of 3.5% NaCl. Two different alloys were used and the results are shown in Figure 7. Alloys UNS S31600 and UNS 32550 were subjected to CPP in 3.5% NaCl with and without the addition of clean Sand at  $24^{\circ}\text{C}$ . No rotation was used in the current experiment. Figure 7 shows that an increase in passive current of the DSS (UNS 32550) due to the addition of the sand does not lead to pitting corrosion at the test temperature. It is also shows that when the same test is performed on the uncoated 316 sample (UNS S31600), the pitting potential of the steel shifts to more negative potential (approximately  $120\text{ mV}_{\text{SCE}}$ ). These results are relevant for the next set of experiments carried out with rotation (see below).

### **Rotational Abrasion Testing and Corrosion Monitoring**

Figure 8 shows experimental setup used in these types of experiments. The authors manufactured a rotational drive shaft that is capable to rotate the rods at 5 variable speeds between 12,100 rpm and 22,100 rpm. However, for simplicity, the authors have chosen two different speeds (minimum and maximum) to study the effect of the rotational speed in an environment containing 3.5% NaCl and sand (see Figure 9). In these experiments, the potential of the sample was monitored between the sample rod and the saturated calomel electrode (SCE), while the current was collected between the rod and a graphite counter electrode using a picoammeter. It is important to mention that neither the calomel electrode nor the graphite rod suffered any damage or contamination during the experiments. Both of them were inspected before and after each of the experiments.

Figure 10 shows the current and potential response for carbon steel double coated (with epoxies A + B) during the abrasion testing. The plot shows two different axes against time, being potential (against the SCE) in the left and current (in microAmps) in the right. Initially, all the experiments were left to equilibrate with the solution containing the 3.5% NaCl and the sand (no rotation was

applied to the sample) for approximately one hour. In this one hour (without rotation), the sample showed a baseline initial current not exceeding 4 nanoAmps (very stable), indicative of a passive system well protected by the coating. At the same time, the potential measured was stable around +180 mV. This potential (when compared to the 316 SS sample showed in Figure 7) is around the passive region for most stainless steels (in good agreement with the 4 nanoAmps currents measured). After establishing the baseline responses of the coated material, the motor is initiated and set to the lowest setting 12,100 RPM. As the motor starts to rotate, the current remained constant (and low) and the potential remained at the same value for approximately 10 minutes. At that point, the potential showed a sudden increase to approximately +200 mV followed by a shift in the negative potential (simultaneously with an increase in the current). This change in the current and the potential measured yielded stable values (after several minutes) of current (~300 microAmps) and potential (-200 mV). However, the fact that the current did not increase to higher values and that the potential did not shift to a more negative value suggest that the coating has been compromised, but not catastrophically failed. This 'quasi-re-passivation' behaviour was observed after 15 minutes from the beginning of the coating breach. The quasi-re-passivation behaviour was disrupted by increasing the rotation rate from 12,100 rpm to 22,100 rpm, which leads to a relatively slow (about 10 minutes) increase in the current, from 310 microAmps to 850 microAmps at the maximum 22,100 rpm (see Figure 10). However, the potential did not change significantly during the 30 minute maximum rotation (essentially remained constant at about -200 mV). At the end of the maximum rotation speed (between 140 and 150 minutes), again a repassivation behaviour was observed. As soon as the rotation was removed (at 150 minutes in Figure 10), the current increased to ~3000 microAmps and the potential shifted to a very negative value of almost -600 mV. One important feature of these experiments is that the high speed rotation did not interfere (or cause an increase in the noise of the electrochemical signals measured). Additionally, the fact that the coating is compromised but the current does not increase during the time when the sample is rotating is unexpected. However, Uhlig<sup>11</sup> observed similar results when studying the corrosion rates of carbon steels at 4000 rpm. Uhlig proposed that these results are explained by an initial inhibiting effect of oxygen on the corrosion rate (more oxygen is injected into the solution as the rotational speed is increased). In Uhlig's view, the potential measurements confirmed that small amounts of oxygen increase the anodic polarization probably by adsorption on anodic sites. Higher concentrations of oxygen caused depolarization of cathodic areas accompanied by an initial increase of the current that lead to a "quasi-repassivation" behaviour. Uhlig also pointed out that ferric ions (in solution) may also act as an inhibitor or depolarizer depending on surface concentration.

Similar experiments (to those shown in Figure 10) were conducted with the carbon steel coated with epoxy A (as shown in Figure 11) and with Cr-coated and epoxy A coated steel (shown in Figure 12). In both cases, the similar trend as noted above was observed. It is important to notice that the Cr-coated steel showed very similar behavior as the carbon steel. This is most likely to the fact that the abrasion of the particles first removed the epoxy coating and subsequently partially remove the Cr coating (in some localized areas), leading to a corrosion attack very similar to that observed for the carbon steels tested in the same fashion.

In the case of the 303 austenitic steel coated with epoxy A, during the abrasion testing (shown in Figure 13), the potential did not shift towards the negative direction (as in the case of the carbon and Cr-coated steels). Furthermore, the current measured during the abrasion test were in the order of 100 microAmps or less (quite low compared to the carbon and Cr-coated steels). However, this is expected since the austenitic steels should repassivate in this environment at this temperature. The most remarkable feature of this experiment is the change in current when the sample rotation is increased from 12,100 rpm to 22,100 rpm. It looks like that the current transients become larger in current but shorter in time and frequency. This is most likely due to the fact that the active sites in

the 303 austenitic steels were already consumed during the initial test at the lower rotational speed. Another interesting feature of this experiment is that the measured potential was always positive (moving towards +100 mV) regardless of the rotation speed. Although we still do not understand why the potential changed without any rotation for 20 minutes and then suddenly recuperated (following the same trend towards the +100 mV). This steady increase in the potential may indicate that even when the coating is compromised in localized areas (by pinholes or cracks), the overall sample can readily repassivate and continue to move towards positive values. The final interesting point in this experiment is that at the end of the rotation there is a transient in current that did not last too long. Concurrently, there was a shift in the potential towards a negative value, but then it repassivated (as the current remained low).

The 316 austenitic steel coated with Epoxy A, showed an interesting profile. The initial reading during the rest conditions showed very low current (nanoAmps) and a stable potential moving from +100 mV towards +200 mV (shown in Figure 14). However, when the rotation started, the potential shifted towards a negative potential of -200 mV (very similar to the case of the carbon and Cr-coated steels) and the current increased steadily to +300 microAmps (quite high for an austenitic stainless steel). Because of this high current and low potential, the experiment was stopped and the sample was inspected. Opposite to the 303 austenitic steel, the coating had come out and a crevice type like corrosion was found at the bottom of the cylinder (where the coating had felled apart).

Figure 15 shows a picture of the different cylinders studied (before and after testing). Of particular interest is the fact that in all cases, the steel showed localized areas where corrosion was present (underneath the coating). This suggests that the coating does not fail catastrophically (except for the case of the 316 coated samples). It appears that the impingement of the particles in the coating allows for some defects to be created. However, such defects apparently do not grow rapidly; possibly because the rotation speed impedes their growth (not allowing fresh solution to penetrate through the pore). Additionally, this may be the result of a “synergistic” effect between the rotation and the repassivation of the steel due to an increase in the oxygen content in the mixture (as pointed out by Uhlig in 1964!). From all the samples studied, the 303 austenitic steel coated with epoxy A is the best option (at least for the conditions in the present study).

### **Critical Temperature in MEG and water**

An additional experiment was also conducted on two 304 SS coated with epoxy A, exposed to a mixture of 90% MEG and 10% DI H<sub>2</sub>O (shown in Figure 16). This experimental condition simulates those conditions found under down-hole operational conditions. In order to accelerate the degradation of the protective epoxy coating (epoxy A) and expose the underlying substrate (304 SS in this case), the samples were subjected to a ZRA-type experiment (two identical electrodes). The potential between the couple and a pseudo-reference electrode (Ag/AgCl wire) was monitored concurrently with the current between the two epoxy-coated 304L SS samples (with similar exposed areas). Initially, the potential and the current were recorded while the temperature of the system was constant (at 22.5°C). The current fluctuated below 10 nanoAmps (which seems to be a very low current). However, the transients were accompanied by transients in the potential between values ranging from -350 mV to -400 mV. However, no significant breakdown of the coating (or increase of the current) was observed at this stage of the test. As the temperature is increased from 22.5°C towards 100°C at a rate of 0.5°C/min (very similar to the ZRA test explained above), current transients develop. As the temperature arrived to 30°C, the current transients still occurred, but the potential started to drop steadily towards -500 mV. Apparently, as the temperature was increased to higher values, the coating started to detach from the steels but no significant increase in the current was observed (although micro crevices may have formed in the interface of the uncoated areas with

those areas coated, which may have shifted the potential to lower values). At 93.5°C, the current abruptly increased and the potential started to recuperate. This may suggest that the coating failed catastrophically at this critical temperature (93.5°C). By monitoring the current and potential at this constant temperature, it was observed that the potential gradually started to repassivate and the current remained stable (again, a possible sign of passive behaviour by the suddenly uncoated steel). It is important to notice that the samples were not rotated in this part of the work. Further work will aim at testing the epoxy coated steels (hopefully with better coatings) under these conditions at different temperatures.

## CONCLUSIONS

In the present work, the development of two novel methodologies to assess the pitting corrosion and wear resistance of steels exposed to aggressive environments are described.

The first method (a modified version of the ZRA testing) is not only measured accurately (within 1°C) the Critical Pitting Temperature (CPT) on the different alloys studied, but also allowed to perform the testing in a very short time. This technique is a promising way to characterize and rank different materials subjected to the same environmental conditions.

The second method consisted in the testing of coated steels at high speed rotations to simulate the environment in down-hole environments. As expected, the carbon steels presented very high currents (thousands of microAmps) once the coating was compromised (after the rotation started). Similarly, the stainless steels (SS) type 303 and 316 showed high currents (hundreds of microAmps) once the coating was compromised (after the rotation started). However, the epoxy coating A had better adhesion to the 303 steel (compared to the 316 steel). When the same coating (Epoxy A) was applied to 304 SS and the sample was exposed to a mixture of 90% Mono-Ethylene Glycol and 10% DI H<sub>2</sub>O (without rotation) at higher temperatures, the coating failed at a critical temperature of 93.5°C. Ongoing work is aiming at understanding what is the critical temperature and rotational speed for these types of coatings in the presence of the MEG:DI water with addition of particles (which is more representative of the downhole type of environments).

## ACKNOWLEDGEMENTS

The authors wish to thank Dr. Oliver Moghissi and Steve Waters for valuable discussions.

## REFERENCES

- 1 ASTM G48 - 03 Standard Test Methods for Pitting and Crevice Corrosion Resistance of Stainless Steels and Related Alloys by Use of Ferric Chloride Solution.
- 2 D. E. Williams, J. Stewart, and P. H. Balkwill; The nucleation, growth and stability of micropits in stainless-steel. *Corros. Sci.* 36 (7), p. 1213-1235 (1994).
- 3 N. J. Laycock, M. H. Moayed, and R. C. Newman. Metastable Pitting and the Critical Pitting Temperature. *J. Electrochem. Soc.* 145, p. 2622 (1998).
- 4 V. M. Salinas-Bravo and R. C. Newman, An alternative method to determine critical pitting temperature of stainless steels in ferric chloride solution. *Corros. Sci.* 36 (1), p.67 (1994).
- 5 ASTM G150 - 99(2004) Standard Test Method for Electrochemical Critical Pitting Temperature Testing of Stainless Steels.

6 ASTM G170-01a, Standard Guide for Evaluating and Qualifying Oilfield and Refinery Corrosion Inhibitors in the Laboratory, ASTM International (2001).

7 ASTM G119-93, Standard Guide for Determining Synergism Between Wear and Corrosion, ASTM International (1998).

8 L. F. Garfias Mesias, J. M. Sykes and C. D. S. Tuck, Effect of Phase Compositions on Pitting Corrosion of 25 Cr Duplex Stainless Steel in Chloride Solutions, Corrosion Science, 38, p.1319, (1996).

9 L. F. Garfias-Mesias and J. M. Sykes, Metastable Pitting in 25 Cr Duplex Stainless Steel, Corrosion Science 41, p. 959 (1999).

10 H. Tsapraillis, M. Iannuzzi, B. Tossey and L. F. Garfias-Mesias, "A Novel Approach for Assessing Corrosion of Cladded Carbon Steels for Marine and Saltwater Applications". 214th ECS Meeting, Honolulu, Hawaii, October 12-17, 2008. Symposium D3: Corrosion in Marine and Saltwater Environments 3.

11 Z. A. Foroulis and H. H. Uhlig, Effect of Velocity and Oxygen on Corrosion of Iron in Sulfuric Acid, J. Electrochem. Soc., Volume 111, Issue 1, pp. 13-17 (1964).

**Table 1. Typical Composition of Stainless Steels used in the Zero Resistance Ammeter (ZRA) test**

<b>Sample</b>	<b>UNS</b>	<b>Fe</b>	<b>Cr</b>	<b>Ni</b>	<b>Mo</b>	<b>N</b>	<b>Cu</b>	<b>Mn</b>	<b>Si</b>	<b>C (max)</b>	<b>S (max)</b>	<b>P (max)</b>
22 Cr DSS	S32205	Bal	21.50	5.70	3.00	0.17	0.00	N/A	N/A	0.05	N/A	N/A
25 Cr DSS	S32550	Bal	24.65	6.08	2.98	0.20	1.63	0.91	0.47	0.03	0.05	0.03
25 Cr DSS	S32750	Bal	24.84	6.93	3.84	0.27	0.08	0.46	0.35	0.01	0.00	0.02
25 Cr DSS	S32760	Bal	25.00	7.00	3.50	0.25	0.75	1.00	1.00	0.05	0.01	0.03

**Table 2. Steels used for the rotating studies in 3.5% NaCl with Saturated Sand**

	<b>COATING</b>
1018 Carbon Steel	Epoxy Coating A
1018 Carbon Steel	Epoxy Coating A + Epoxy Coating B
Cr-Coated Steel	Chrome Coated + Epoxy Coating A
303 Stainless Steel	Epoxy Coating A
316 Stainless Steel	Epoxy Coating A

**Table 3. Critical Pitting Temperature of Stainless Steels used in the Zero Resistance Ammeter (ZRA) test**

<b>Sample</b>	<b>UNS</b>	<b>CPT (°C)</b>
22 Cr DSS	S32205	53
25 Cr DSS	S32550	62
25 Cr DSS	S32750	71
25 Cr DSS	S32760	86

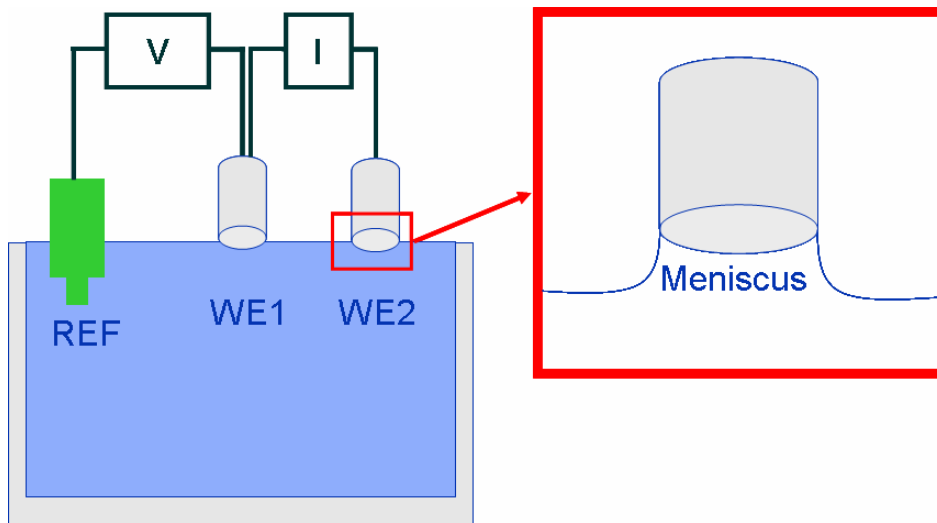


Figure 1. Modified Zero Resistance Ammeter test.

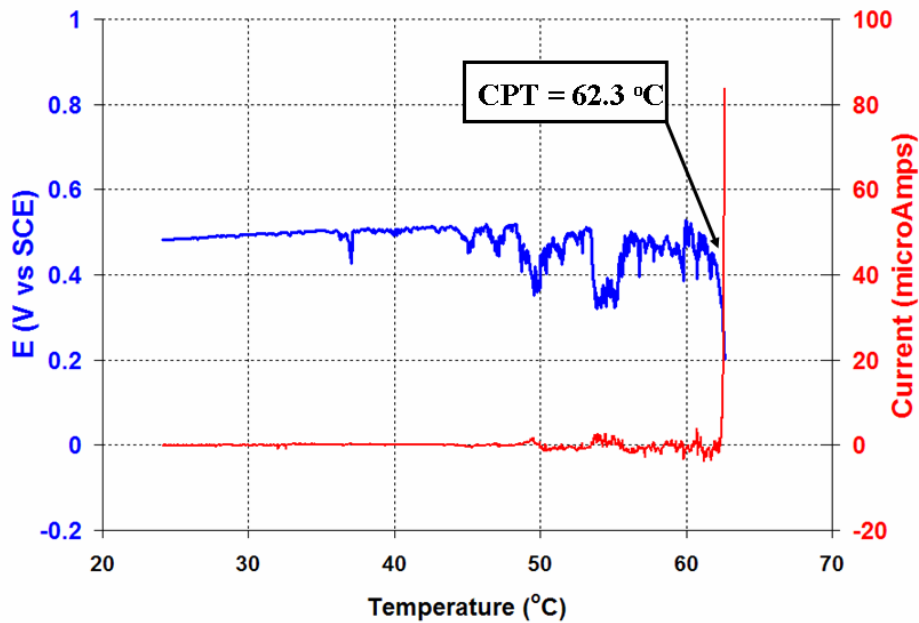


Figure 2. CPT of 25 Cr DSS, UNS S32550.

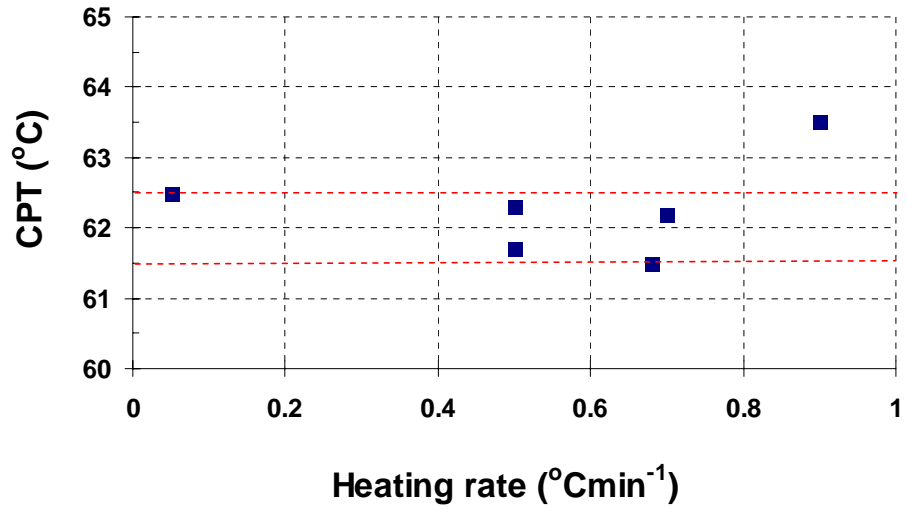


Figure 3. CPT of 25 Cr DSS, UNS S32550 obtained at different heating rates.

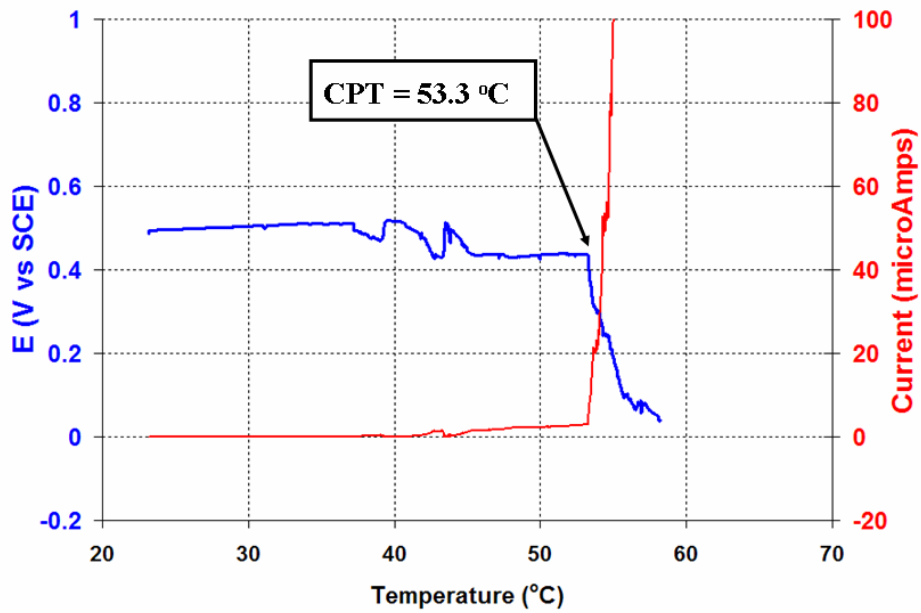


Figure 4. CPT of 22 Cr DSS, UNS S32205.

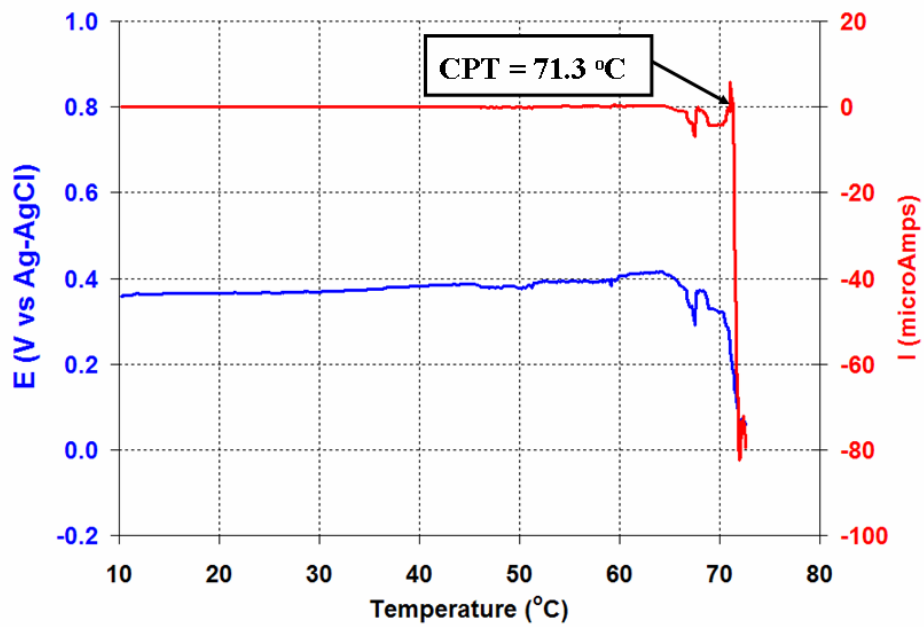


Figure 5. CPT of 25Cr DSS, UNS 32750.

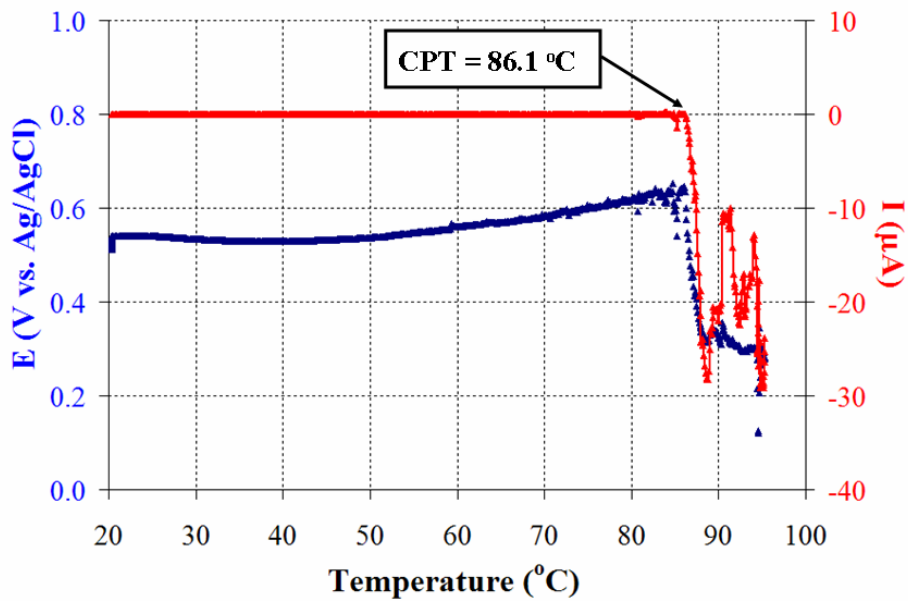


Figure 6. CPT of 25 Cr DSS, UNS 32760.

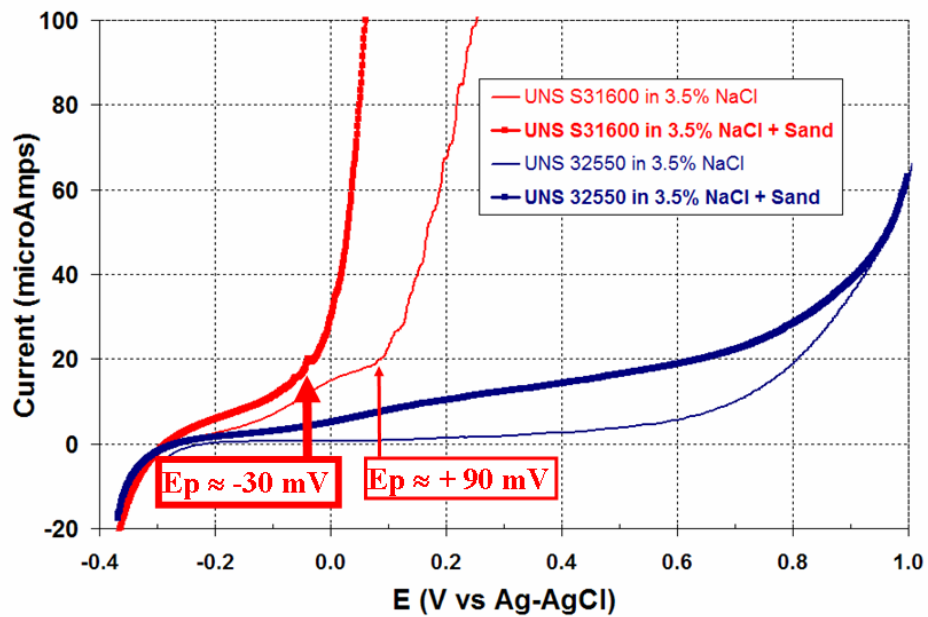


Figure 7. Anodic Polarization of UNS S31600 and UNS 32550 in 3.5% NaCl and Sand at 24°C.

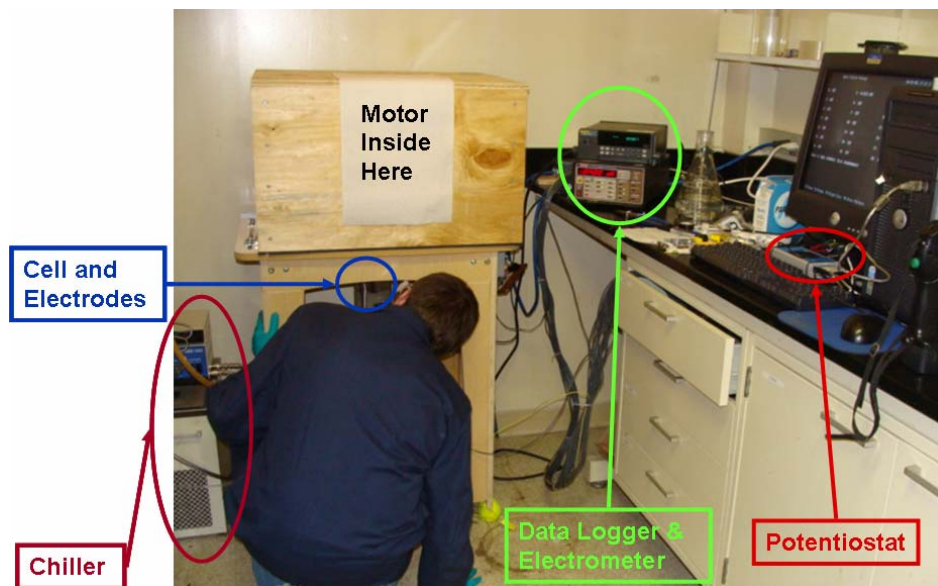


Figure 8. Experimental Design for Abrasion Experiment in 3.5% NaCl and Sand (24°C).

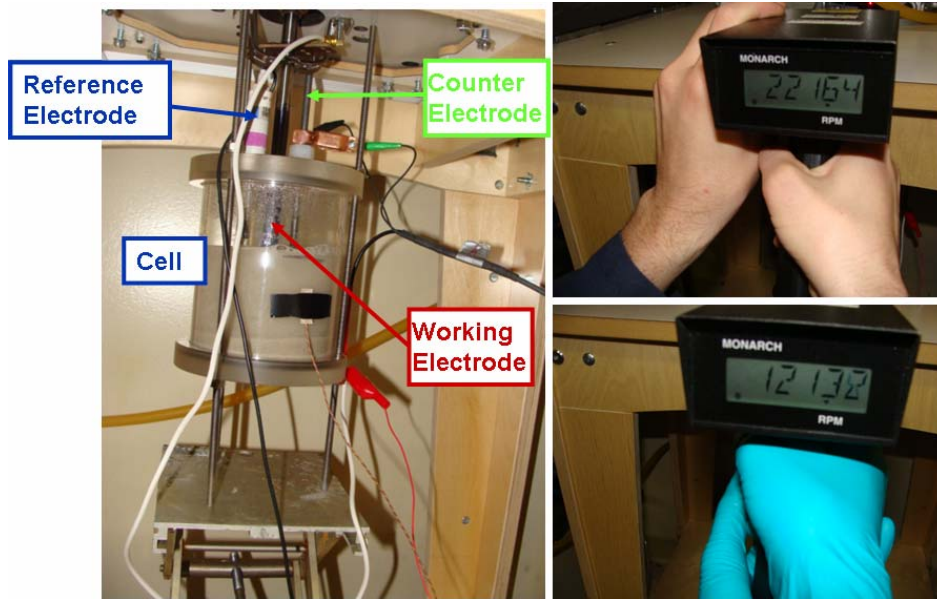


Figure 9. Experimental Design Cell together with Maximum & Minimum Rotation Speeds.

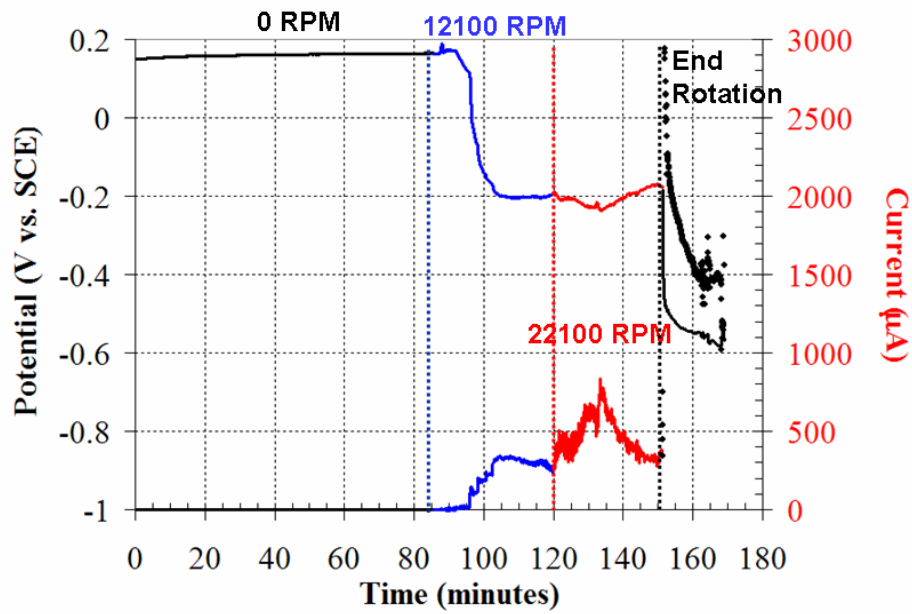


Figure 10. Current and Potential Response for Carbon Steel Coated (Epoxy A + B) during Abrasion Testing.

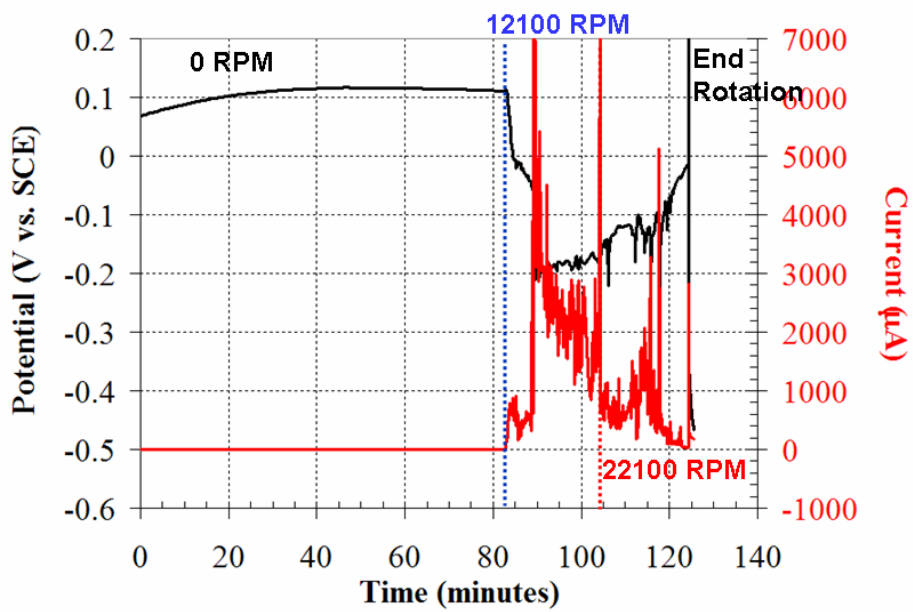


Figure 11. Current and Potential Response for Carbon Steel Coated (Epoxy A) during Abrasion Testing.

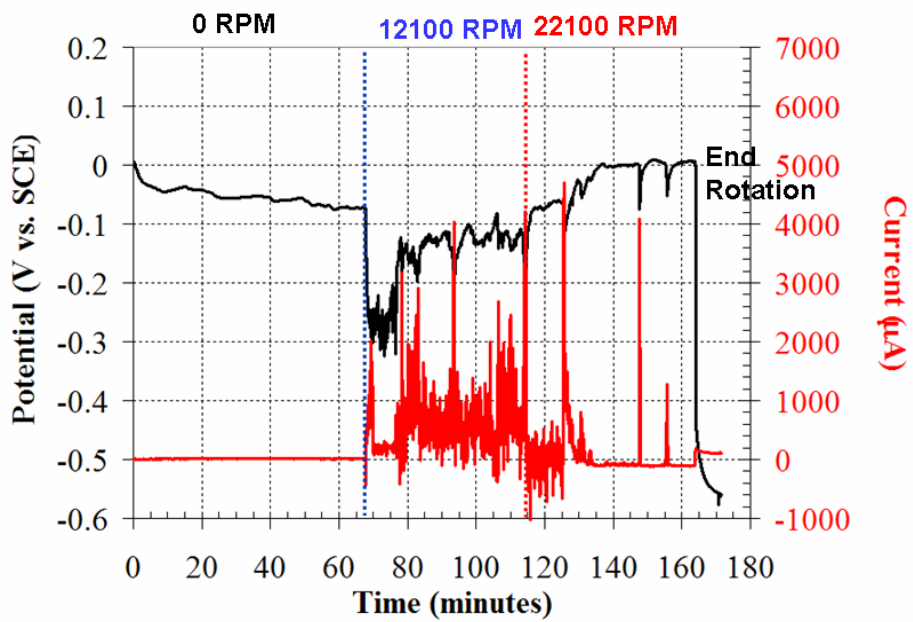


Figure 12. Current and Potential Response for Cr-Coated Steel Coated (Epoxy A) during Abrasion Testing.

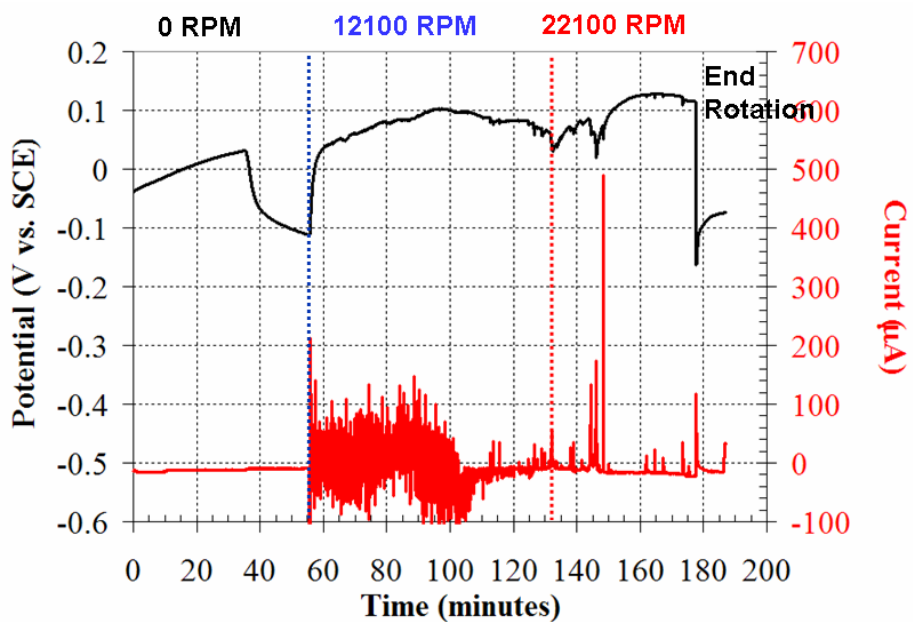


Figure 13. Current and Potential Response for 303 Steel Coated (Epoxy A) during Abrasion Testing.

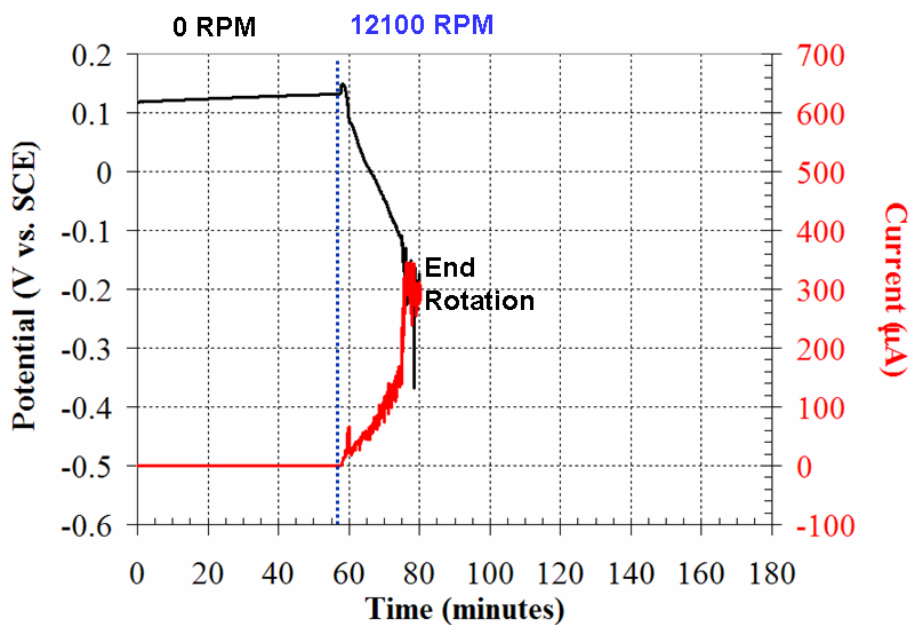


Figure 14. Current and Potential Response for 316 Steel Coated (Epoxy A) during Rotation Experiment.

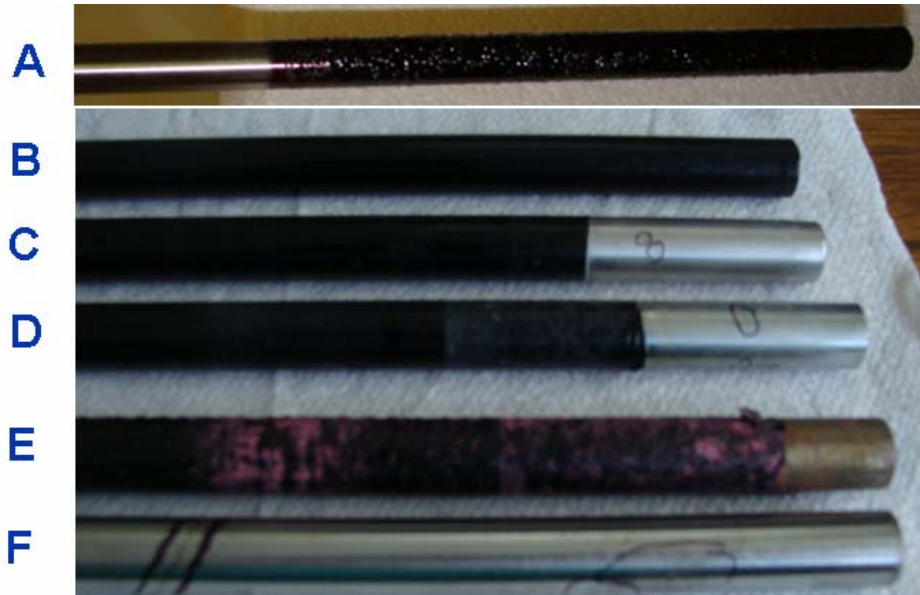


Figure 15. Optical images of samples tested.

- A) Carbon Steel Coated with Epoxy A + Epoxy B (prior to testing)
- B) 316 SS prior to testing
- C) 303 SS after testing (pits circled in the image)
- D) Cr-Coated Steel after testing (pits circled in the image)
- E) Carbon Steel Coated with Epoxy A + Epoxy B after testing (corrosion shown in the uncoated sample)
- F) Carbon Steel Coated with Epoxy A after testing (the coating was removed to image the corrosion sites)

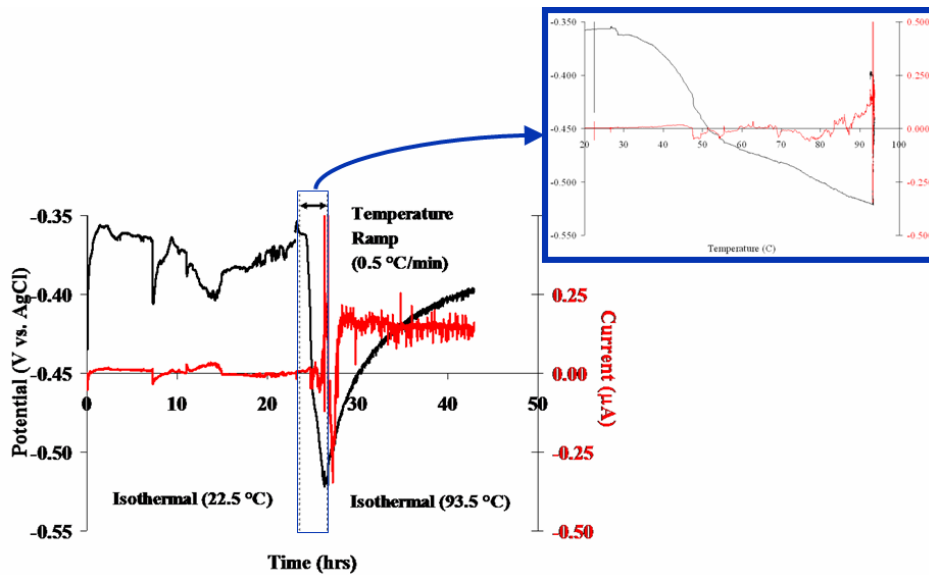


Figure 16. 304 SS Coated (Epoxy A) Exposed to 90:10 MEG:H<sub>2</sub>O Mixture (no rotation)